

Nitrogen Fixation and NO Conversion using Dielectric Barrier Discharge Reactor: Identification and Evolution of Products

Xiaolong Tang¹ · Jiangen Wang¹ · Honghong Yi¹ · Shunzheng Zhao¹ · Fengyu Gao¹ · Chao chu¹

Received: 22 October 2017 / Accepted: 5 February 2018 / Published online: 9 February 2018
© Springer Science+Business Media, LLC, part of Springer Nature 2018

Abstract The recombination (synthesis and conversion) of nitric oxide was investigated using dielectric barrier discharge reactor at atmospheric pressure. In this work, products identification and its evolution of different gas components have been studied. In the NO/O₂/N₂ systems, nitric oxide (NO) can be removed via chemical oxidation and chemical reduction, and corresponding products are NO₂ and N₂, respectively. In the O₂/N₂ systems, N₂O₅ producing from the interaction of NO₃ with NO₂ was also observed. There is an optimum SED at which the highest NO_x yield and best NO conversion efficiency will be achieved. In the H₂O/O₂/N₂ systems, the formation of NO₂, HNO₂ and HNO₃ were observed in both NF and NO conversion. The N₂O molecule, as a byproduct of plasma chemical reaction, was observed in all the experiments when the H₂O or O₂ is presence in the simulated gas. The lowest energy cost of NO conversion is achieved at the SED of 1250 J/L.

Keywords Interconversion · Non-thermal plasma · Specific energy density · HNO₂ · N₂O

Introduction

Nitrogen oxide (NO_x), which represents both NO and NO₂, is one of the main causes of some environmental problems such as acid rain, photochemical smog, and stratospheric ozone chemistry. On the other hand, the increasing demand from the global population will intensify the demand of nitrogen fixation, which will supply the energy for all life on the Earth. For the past few decades, a great deal of interest has been expressed to the analysis of the role of non-thermal plasma (NTP) in different reaction systems involving NO synthesis [1] and NO conversion [2]. The sequence of transformations of initial reactive

✉ Honghong Yi
yhhtxl@163.com

¹ Department of Environmental Engineering, School of Energy and Environmental Engineering, University of Science and Technology Beijing, Beijing 100083, China

species and electric energy into products and thermal energy is usually referred to as the mechanism of the plasma-chemical process. Collision between energetic electrons and substrate molecules (N_2 , O_2 and H_2O) create a mix of reactive species including reactive nitrogen species (RNS: N , NH and $N_2(A^3\Sigma_u^+)$) and reactive oxygen species (ROS: O , HO , HO_2 and O_3) [3, 4]. Evolution of NO in NTP process involves: (1) reactions between NO and reactive species; (2) reactions between different reactive species. Dielectric barrier discharge (DBD) is a prominent technology to generate NTP under a moderate operating condition (atmospheric pressure and room temperature) [5]. Competition with the conventional chemical techniques for NF (Haber–Bosch) and $DeNO_x$ (Selective catalytic reduction, three-way catalyst) motivated a long history research and development effort to increase the product yield and energy efficiency of DBD process. All these efforts are focus on reaction kinetics [4, 6], operating parameters [3, 7] and plasma catalysis [1, 8–10]. Consequently, the evolution characteristics of NO involving production and loss is an interesting subject for DBD process.

NO synthesis using DBD process has been studied extensively [6, 8, 11]. The production of NO from molecular nitrogen is extremely energy intensive due to the large bond strength of nitrogen (945 kJ mol^{-1} or 9.79 eV). Breaking the bond can proceed efficiently via reactions of vibrationally-excited nitrogen molecules ($N_2^*(\text{vib})$). NO synthesis in NTP are controlled by an endothermic step involving $N_2^*(\text{vib}): O(^3P) + N_2^*(^1\Sigma_g) \rightarrow NO + N$, following by a secondary exothermic process: $N + O_2 \rightarrow NO + N$ [11, 12], which is known as the Zeldovich mechanism. The electronically excited species, $N_2(A^3\Sigma_u^+)$, plays the most important role in NO production. Energy stored in $N_2(A^3\Sigma_u^+)$ may be consumed to overcome the high activation barriers of dinitrogen reactions. Teodoru et al. [6] presented a numerical model for N_xO_y remediation in humid air involving ~ 540 reactions. NH radicals combined with $N_2(A^3\Sigma_u^+)$ play a key role in NO synthesis. O , N , OH and HO_2 play a role in both NO production and NO conversion.

DBD has been intensively investigated to eliminate NO in the exhaust gas stream since 1990s [2, 3]. Penetrante et al. [3, 7, 13] propose that the electron mean energy in the DBD reactor is weakly dependent on reactor parameters under identical gas composition and temperature. The performance of DBD reactor for NO conversion are mainly dependent on energy consumption and gas composition. For DBD in $H_2O/O_2/N_2$ system, NO is mainly oxidized to NO_2 and HNO_2 by O and OH , respectively [3, 14, 15]. Jōgi et al. [16] proposed that the presence of back-reaction $NO_2 + O \rightarrow NO + O_2$ leads to the saturation of NO oxidation in O_2/N_2 system. NTP generated in gas with oxygen shows high oxidative potential, which is beneficial for the conversion of NO to NO_2 .

Investigation of NF and NO removal in DBD reactor, even for a system as simple as $H_2O/O_2/N_2$, requires a reaction mechanism involving many species such ions, atoms, radicals, and molecules. Among all of the plasma chemical reactions, which one is the dominant reaction depending on the quantity of active species and the reaction rate involving these species. The co-existence of reactive species for NO formation and loss make DBD chemistry such a complex system. Effects of energy input and gas composition on the performance of DBD chemical process are the most industrial interests. However, there are no systematic studies on NO formation and loss in one investigation.

Present study is devoted on investigation of the effect of SED and gas composition on NO evolution and byproducts formation in DBD process. The simulated gas has been introduced into the DBD reactor with a constant flow rate under the ambient temperature and pressure. In “Energy Consumption and of DBD System” section, the effect of gas composition on electrical characterization has been investigated. In the next two sections,

the performance of DBD reactor was investigated in six different systems: (1) NO synthesis in O_2/N_2 , H_2O/N_2 and $H_2O/O_2/N_2$ systems (“NO Formation in DBD System” section); (2) NO removal in $NO/O_2/N_2$, $NO/H_2O/N_2$ and $NO/H_2O/O_2/N_2$ systems (“NO Conversion in DBD System” section). Finally, a comparison of NO_x and N_2O concentration as a function of SED with and without initial NO was investigated in “ NO_x Evolution and N_2O Production” section.

Experimental Setup

The schematic of the experimental setup is shown in Fig. 1. NTP was obtained in a coaxial cylinder-type DBD reactor energized by a high-voltage power supply. The discharge gap is fixed at 2 mm with a total discharge volume of 2.5 mL. Gas composition and flow rate were controlled by mass flow controllers (MFC). Water vapor was added to the feed by bubbling N_2 through an H_2O saturator kept at 303 K. A total flow rate of 0.3 ± 0.01 L/min, which was equal to a residence time of 0.5 s, was maintained in DBD stage. Six different systems were used to investigate the effect of oxygen and water vapor on DBD performance, as shown in Table 1.

Electrical Characterization

The power supply employed in the experiments delivered a sinusoidal AC output voltage of up to 20 kV, with frequency varying from 5 to 20 kHz. The output ac voltage was applied to the stainless steel rod in the reactor and measured by using a capacitive divider

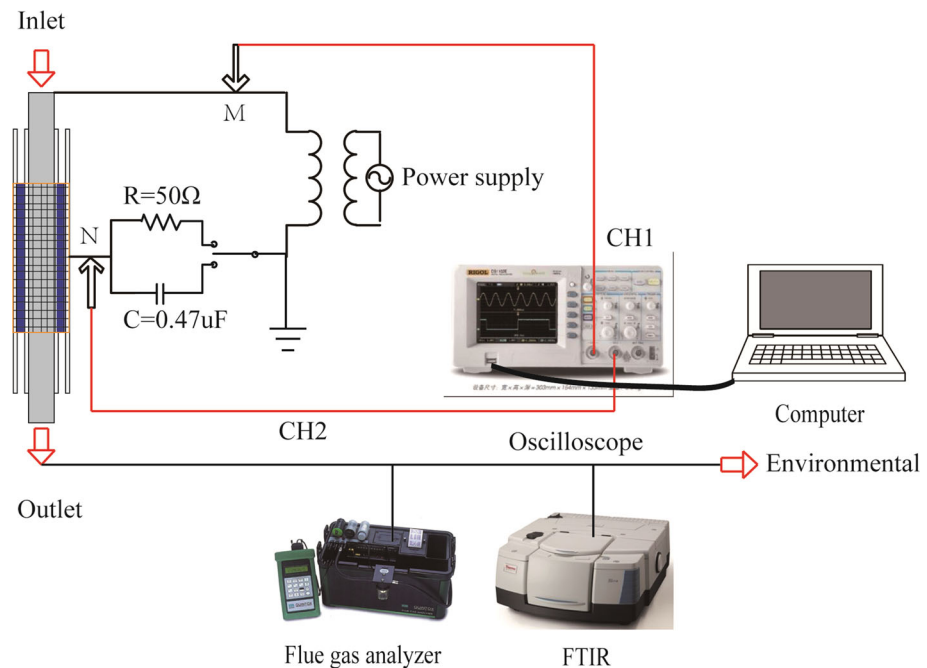


Fig. 1 Schematic of the experimental system

Table 1 Specifications of the gases used

System	Name	Specification
E-1	O ₂ /N ₂	6.0% O ₂ , balance N ₂
E-2	NO _x /O ₂ /N ₂	495 ppm NO, 80 ppm NO ₂ , 6% O ₂ , balance N ₂
E-3	H ₂ O/N ₂	3.8% H ₂ O(g), balance N ₂
E-4	NO _x /H ₂ O/N ₂	467 ppm NO, 67 ppm NO ₂ , 3.8% H ₂ O(g), balance N ₂
E-5	H ₂ O/O ₂ /N ₂	6% O ₂ , 3.8% H ₂ O(g), balance N ₂
E-6	NO _x /H ₂ O/O ₂ /N ₂	458 ppm NO, 50 ppm NO ₂ , 6% O ₂ , 3.8% H ₂ O(g), balance N ₂

(1000:1), where the wave form of the sinusoidal ac voltage is displayed on the oscilloscope. The other electrode made of copper mesh (20 mesh) was grounded through either a charge-probe capacitor $C_m = 0.47 \mu\text{F}$ or a resistor $R = 50 \Omega$ in series with a switch as shown in Fig. 1. The discharge power of the DBD reactor was determined from the enclosed area of Lissajous figure. The specific energy density in joules/liter (J/L) was calculated using the formula:

$$\text{SED (J/L)} = \frac{P}{Q}$$

where the P is the discharge power calculated from V–Q Lissajous figure (J/s), Q is the flow rate of gas in L/s.

Chemical Analysis

The concentration of NO, NO₂ and N₂O was analyzed online by Nicolet iS50 Fourier transform infrared (FTIR) spectrometer (Nicolet iS50, Thermo Fisher scientific, America, pathlength is 2.4 m) operation in the adsorption mode, with a resolution of 4 cm⁻¹. Characteristics features were obtained for NO₂ in the range of 1660–1540 cm⁻¹ [17], for NO in the range of 1980–1860 cm⁻¹ [1, 17], for N₂O in the range of 2270–2140 cm⁻¹ [18] and for O₃ the range was 1080–940 cm⁻¹. The above chosen wavenumber ranges provided signature FT-IR plot characteristic of each molecular species, and obey the Beer–Lambert law: $I = I_0 \exp(-\sigma_v NL)$, where σ_v is absorption cross-section, N the molecular density and L the absorption path length. The absorbance of each line was then given by $A = \ln(I_0/I)$. The oxygen content were detected by flue gas analyzer (Kane, KM9106).

The energy cost in mega-joules per mole for the conversion of NO was calculated using the formula:

$$\text{EC}_{\text{NO}_x} (\text{MJ/mol}) = \frac{\text{SED} \times A \times 10^6}{\text{NO}_{\text{inlet}} - \text{NO}_{\text{outlet}}}$$

where NO_{inlet} and NO_{outlet} are the NO concentration of inlet and outlet of the reactor in ppm; SED is the specific energy density (J/L); “A” is a constant equal to 24.5, 1 mol is equal to 24.5 L at 25 °C.

Results and Discussion

Energy Consumption and of DBD System

The DBD geometry designed for this research is a typical coaxial-tube with a double quartz wall and coupled to an ac high-voltage (HV) source, as shown in Fig. 1. The measured probe voltage across the capacitor C_m (0.47 μF) is proportional to the charge crossing the electrode [19, 20]. The measured operating voltage and charge values are plotted against each other in Q–V figures, which are better known as Lissajous figures. Using on period of voltage measured at the point of M and N (Fig. 1), the characteristic V–Q Lissajous curves at applied power of 24 W were plotted (Fig. 2). The energy dissipated for discharge per one cycle at applied power of 24 W is varied between different systems: 1.04×10^{-3} J for the O_2/N_2 , $\text{H}_2\text{O}/\text{N}_2$ and $\text{H}_2\text{O}/\text{O}_2/\text{N}_2$ system at 9.92 kHz; 0.98×10^{-3} J for the N_2 system at 9.80 kHz. The ratio of discharge power to applied power for 9.92 and 9.80 kHz are 43 and 40%, respectively. In presence of H_2O and O_2 , the effect of gas composition on power used to discharge is not obvious at a fixed applied power.

DBD reactor is generally considered as a capacitive load. The slope of the V–Q Lissajous figure before electrical discharge, A–B or C–D, represents capacitance of DBD reactor which is estimated to 7.2 pF. Dielectric capacitance of dielectric tubes (C_d), slope of B–C and A–D, are estimated to 16 pF for plasma on. The results in Fig. 2 show that gas composition has little effect on the capacitance of DBD reactor. Breakdown voltage (U_b), the lowest voltage value at which the gas turn to plasma, can be also obtained from Q–V Lissajous figures. The U_b shows a little decrease with O_2 or H_2O feeding into DBD reactor compared with pure nitrogen plasma. For a power supply with a given voltage and frequency, lower U_b indicate longer discharge duration.

The discharge power of different applied power calculated from Q–V Lissajous figures are shown in Fig. 3. The average discharge power (P_{ave}) of different systems was calculated from the discharge power of DBD reactor at a fixed applied power. Figure 3 (dashed line) shows the calculated P_{ave} of discharge power as a function of applied power. The increase of average discharge power is nearly linear with the applied power increasing

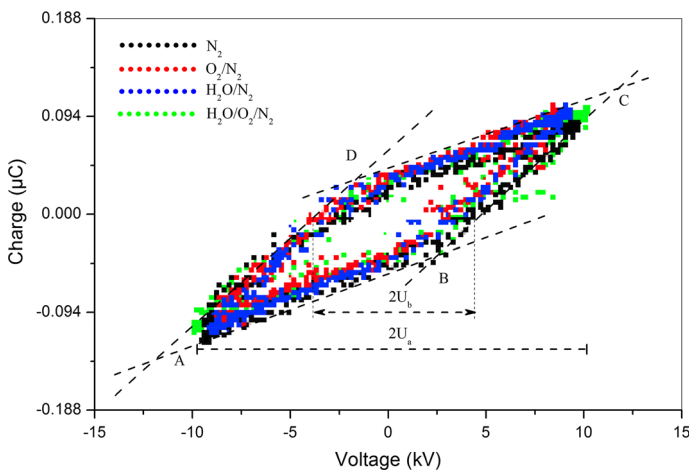


Fig. 2 Typical Q–V Lissajous figure of DBD reactor driven with different simulated gases (applied voltage, $U_a = 10.0$ kV; 9.92 kHz for O_2/N_2 , $\text{H}_2\text{O}/\text{N}_2$ and $\text{H}_2\text{O}/\text{O}_2/\text{N}_2$; 9.80 kHz for O_2/N_2 ; applied power: 24 W)

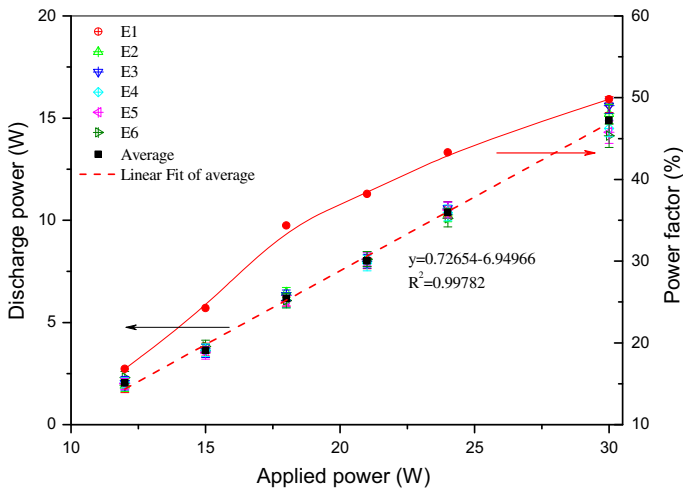


Fig. 3 The discharge power as a function of applied power for different gas component

from 10 to 30 W. The changes of discharge power among different gas components are negligible for a given set applied power lower than 24 W. The ratio of discharge power to applied power increases with frequency decreasing from 10.2 to 9.8 kHz.

NO Formation in DBD System

Identification of N_xO_y and HNO_x by IR Spectroscopy

Figure 4 presents typical FTIR spectra of different systems (O_2/N_2 , H_2O/N_2 and $H_2O/O_2/N_2$) at SED of 2080 J/L. The main products contain NO, NO_2 , N_2O , N_2O_5 , HNO_2 and HNO_3 , and the corresponding spectral performance are listed in Table 2.

In the O_2/N_2 system, NO and NO_2 were observed in the outlet gas by using the FTIR around 1900 and 1600 cm^{-1} , respectively. The limiting step in NO production is the breaking of the strong triple bond of the N_2 molecule (9.77 eV). The NO produced from the chain reaction $O(^3P) + N_2(^1\Sigma_g) \rightarrow NO + N$ and $N + O_2 \rightarrow NO + O$ will be quickly oxidized to NO_2 by O_3 and O [11, 27]. The spectra of N_2O_5 and N_2O were also observed. The spectral behavior of N_2O_5 is very similar to that of N_2O_4 : $\nu_{as}(N-O)$ at 1720–1750 cm^{-1} , $\nu_s(N-O)$ at 1300–1340 cm^{-1} , and $\delta(NO_2)$ at 750 cm^{-1} . In addition, N_2O_5 manifests a band near 860 cm^{-1} , which is different with N_2O_4 . As shown in Fig. 4b (E-1), the band near 860 cm^{-1} combined with band at 1700 and 1320 cm^{-1} may be the spectral behavior of N_2O_5 . The known routes for N_2O_5 formation are via strong oxidation of N_2O_4 by ozone, interaction of NO_3 with NO_2 , or dehydration of HNO_3 [18]. In the O_2/N_2 system, N_2O_5 may be mainly produced from the interaction of NO_3 with NO_2 .

In the H_2O/N_2 system, the main products are NO and NO_2 with small fraction of HNO_2 . The IR behavior of HNO_2 and HNO_3 are similar: 1680–1700, 1260–1300 and 790–820 cm^{-1} for HNO_2 ; 1700, 1300–1330, 880–900 cm^{-1} for HNO_3 . The spectral behavior of HNO_2 and HNO_3 overlap with each other near 1700 and 1300 cm^{-1} . The spectral differences between the two are 790–820 cm^{-1} for HNO_2 and 880–900 cm^{-1} for HNO_3 . As shown in Fig. 4b, the bands at 791 and 853 cm^{-1} are believed to represent the N–O single bond valence vibrations of trans- and cis-tautomerism of HNO_2 molecule, respectively

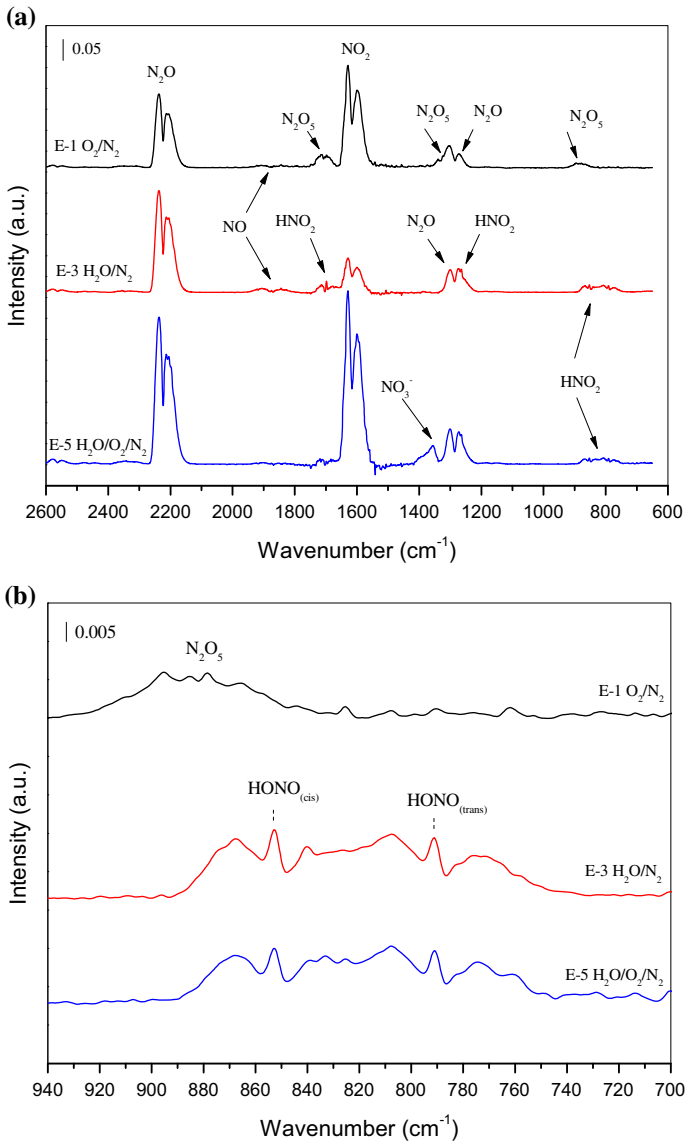


Fig. 4 FTIR spectra of outlet gas streams at the SED of 2080 J/L for NF. **a** 600–2500 cm^{-1} , **b** 700–920 cm^{-1}

(E-3 and E-5). In the case of $\text{H}_2\text{O}/\text{N}_2$ system, the NO can be formed from the reaction between NH radical and hydroxyl radical (OH) [6].

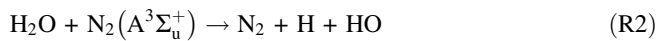


Lowest electronically excited state of N_2 , $\text{N}_2(\text{A}^3\Sigma_u^+)$, and first electronically excited states of N, $\text{N}(\text{}^2\text{D})$, play a key role in the formation of NH and OH [6].

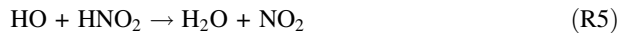
Table 2 IR spectral performance of N_xO_y in gas

Species	IR band (cm^{-1})	Mode	References
NO	1980–1860		[18]
NO_2	1620, 1318, 750	$\nu_{\text{as}}, \nu_{\text{s}}, \text{bend}$	[17]
N_2O	2220, 1280	$\nu(\text{N-N}), \nu(\text{N-O})$	[21]
N_2O_4	1760, 1320, 750	$\nu_{\text{as}}(\text{N-O}), \nu_{\text{s}}(\text{N-O}), \delta(\text{NO}_2)$	[22]
N_2O_5	1720, 1250, 744 (860)	$\nu_{\text{as}}(\text{N-O}), \nu_{\text{s}}(\text{N-O}), \delta(\text{NO}_2)$	[23]
HNO_2	1690, 1260, 800	$\nu(\text{N}=\text{O}), \text{HON bend}, \nu(\text{N-O})$	[24]
HNO_3	1700, 1320, 880	$\nu_{\text{as}}(\text{N-O}), \nu_{\text{s}}(\text{N-O}), \text{O-N-O bend}$	[25]
O_3	2000–2100, 1000–1600		[26]
NO_3^-	1360		[18]

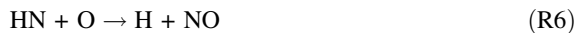
as Asymmetric stretching, *s* symmetric stretching



The HNO_2 and NO_2 in the $\text{H}_2\text{O}/\text{N}_2$ plasma are generated from the reaction [28, 29]:



In the $\text{H}_2\text{O}/\text{O}_2/\text{N}_2$ system, the main products are NO and NO_2 with small fraction of HNO_2 and HNO_3 . NO can be also formed by the reaction [6]:



An additional shoulder at 1698 cm^{-1} , and bands at 1360 and 1314 cm^{-1} were observed, which may be attributed to HNO_3 [30]. Very little information, however, can be found in the literature concerning the quantitative analysis of nitric acid vapor in such gas mixtures. Owing to the reaction of nitrogen oxides with HO, nitric acid vapor (HNO_3) and nitrous acid vapor (HNO_2) can be formed, especially at higher concentrations of nitrogen dioxide [6].



Effect of SED on NO and NO_2 Concentration

NO and NO_2 concentration as a function of SED for different gas compositions (O_2/N_2 , $\text{H}_2\text{O}/\text{N}_2$ and $\text{H}_2\text{O}/\text{O}_2/\text{N}_2$) are shown in Fig. 5. The O_3 was only observed in the O_2/N_2 plasma with the SED below 1600 J/L . The formation of ozone is strongly affected by temperature because of thermal decomposition of ozone, and the formation of NO will further aggravate the depletion of O_3 . For a fixed SED, NO concentration of different

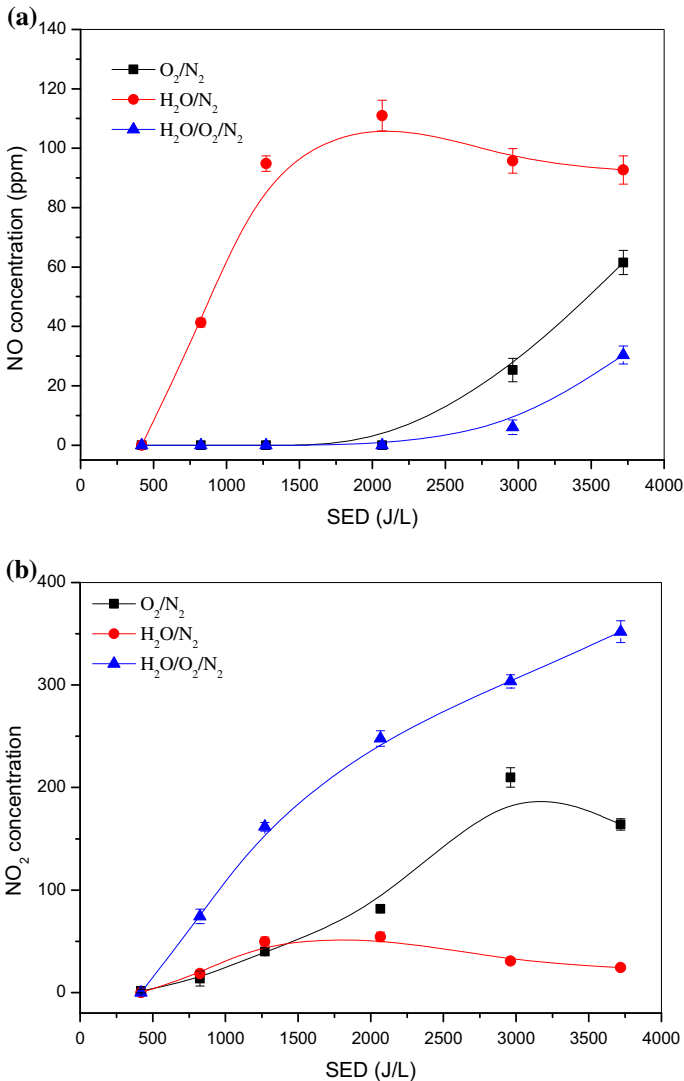


Fig. 5 NO concentration (a) and NO₂ concentration (b) as a function of SED in DBD reactor for NF process

systems are ordered as follows: H₂O/N₂ > O₂/N₂ > H₂O/O₂/N₂. NO₂ concentration of different systems follows the opposite order.

In the O₂/N₂ system, the dissociation of O₂ and N₂ is the main chemical process. The energy cost of O₂ dissociation in atmospheric pressure NTP is 6.0 eV for production of two O atoms in the ground state and 8.4 eV for production of one O atom in the ground state and second in the O(¹D) state [31]. Most of O(¹D) is quenched by O₂ to the ground state O(³P). Since electron mean energy in DBD process is between 3 and 5 eV [7], most of the O atoms in dry air come from the impact with excited electronic states of N₂. It is well known that dissociation energy of oxygen (5.2 eV/O₂) is lower than that of nitrogen

(9.79 eV/N₂) [32]. O₂ dissociation is energetically favorable reaction pathways compared with N₂ dissociation. At low SED, the oxidation of NO to NO₂ is accomplished via R9.



The reactor temperature increases with the increase of SED. It is not favor for NO oxidation, which is an exothermic reaction. A significant amount of the O radicals can reduce NO₂ back to NO:



Therefore, the NO₂ concentration increase firstly then decrease with the increase of SED.

In the H₂O/N₂ system, NO concentration is higher than NO₂ concentration. It is clear that the rate of NO₂ formation from the reaction R4 and R5 involving NO, HO and HNO₂ is slower than that of NO formation. NO concentration increase with SED increasing from 400 to 2000 J/L then decrease with SED further increasing. The reason for this is that the increase of NO concentration and SED will cause product's reaction involving N.



In H₂O/O₂/N₂ system, the increase of NO₂ concentration was nearly linear with the increase of SED from 400 to 3000 J/L in plasma. In the presence of H₂O and O₂, the importance of O(¹D) lies in their high reactive activity with contaminant molecules and their reactions with H₂O to produce HO [6]. NO generated from NTP process will be quickly oxidized to NO₂ and HNO₂.



NO Conversion in DBD System

In NO/O₂/N₂ system, the outlet products are NO and NO₂ with small fraction of byproduct N₂O (Fig. 6, E-2). N₂O₅ formation was not observed in this system. The initial NO will suppress the formation of ozone. NO₃ forms from NO₂ oxidation is also suppressed in the presence of NO. Since N₂O₅ are mainly formed from oxidation of N₂O₄ by ozone and interaction of NO₃ with NO₂, the formation of N₂O₅ would be suppressed with addition of NO. Atomic N and O are two major reactive species which contribute to reduction and oxidation, respectively. NO was mainly oxidized to NO₂ by atomic O at SED of less than 1000 J/L. NO and NO₂ interconvert into each other via reaction NO + O → NO₂ and NO₂ + O → NO + O₂. The increase of O concentration with the increase of SED can improve the back reaction NO₂ + O → NO + O₂, which will reduce the conversion of NO-to-NO₂. As shown in Fig. 7b, NO₂ concentration increase firstly then decrease with the increase of SED in the NO/O₂/N₂ system. NO conversion efficiency increases with SED increasing from 400 to 2000 J/L (Fig. 7). Further increase of SED will reduce the conversion efficiency of NO-to-N₂ due to product's reaction of N₂ and O₂ to form NO. The energy cost of NO conversion increases nearly linear with the increase of SED in NO/O₂/N₂ system (Fig. 9). Limitless increase of SED is not favor for NO conversion due to the interconversion of NO and N₂, NO and NO₂.

The characteristic FTIR spectrum of NO, NO₂, N₂O, HNO₂ and HNO₃ were observed in the NO/H₂O/N₂ system, as shown in Fig. 6 (E-4). NO₂ concentration is smaller than other

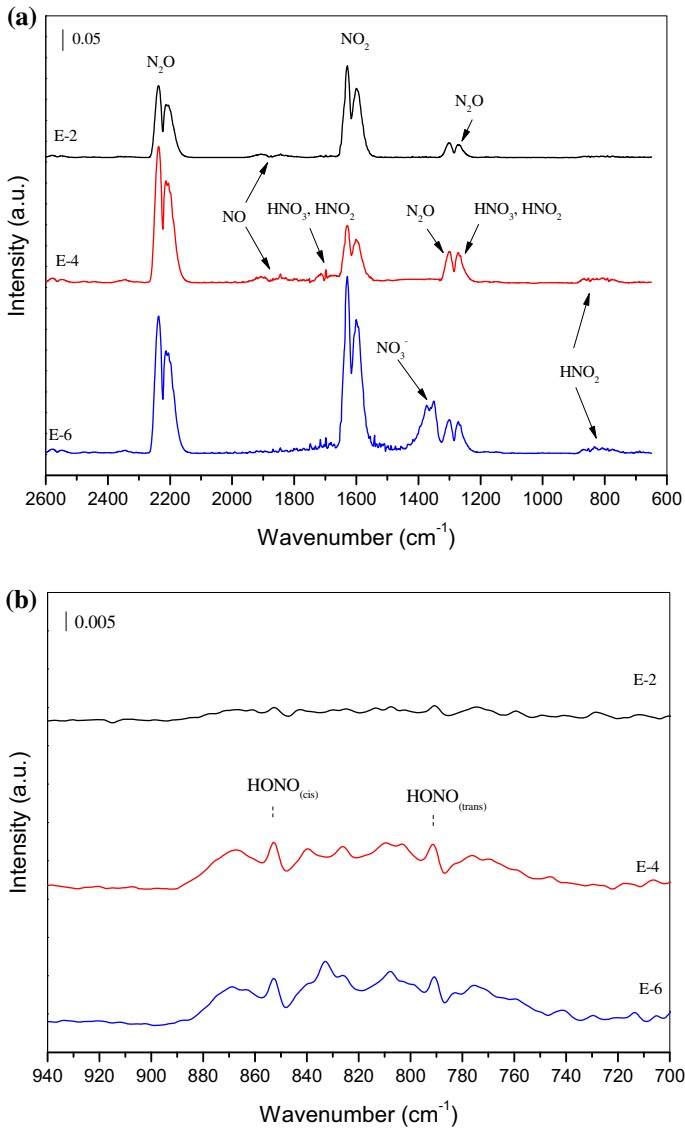


Fig. 6 FTIR spectra of outlet gas streams at the SED of 2080 J/L for NO removal. **a** 700–2500 cm^{-1} , **b** 700–920 cm^{-1}

two systems, which indicates the conversion efficiency of NO-to- NO_2 is lower in NO/ H_2O / N_2 system. The HO and N are main species contribute to NO conversion. The NO-to- NO_2 conversion occur in chain reactions involving HO. Quantitative analysis of HNO_3 vapor in such gas mixtures was not carried out in this work. The relative content of HNO_2 was calculated from the intensity of FTIR spectra from 720 to 910 cm^{-1} . Figure 8 presents the integral area of HNO_2 FTIR spectrum of different systems. The evolution of HNO_2 content with the increase of SED follows the similar trend as the evolution of NO_2 concentration. The NO is oxidized to HNO_2 by OH, further the NO_2 is formed by the reaction HNO_2 with

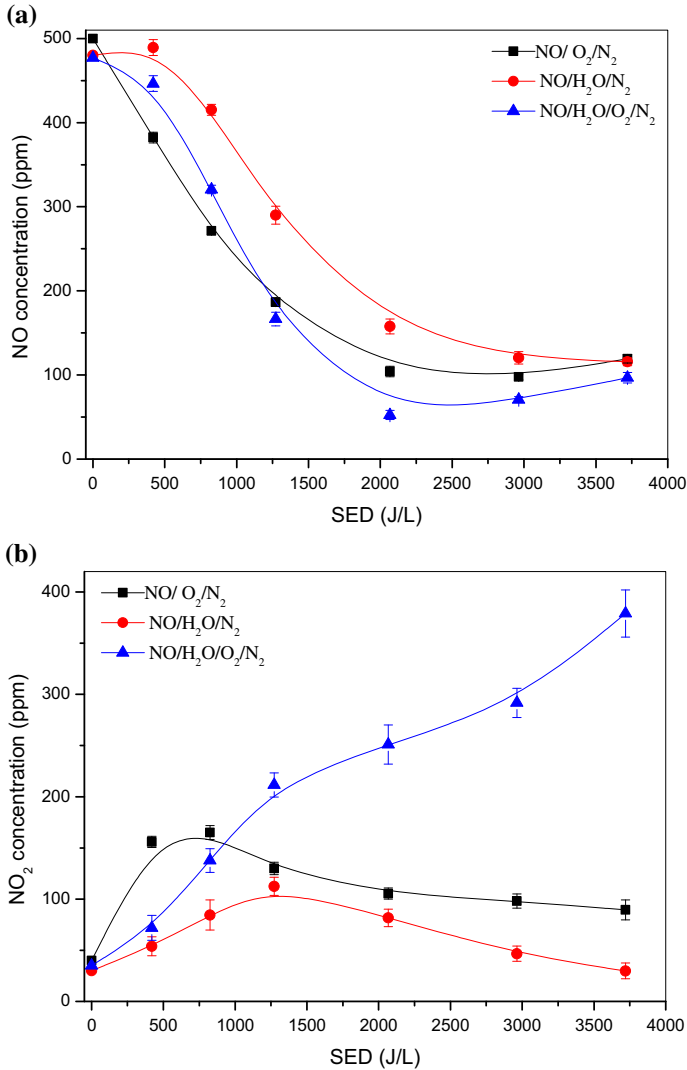


Fig. 7 NO concentration (a) and NO₂ concentration (b) as a function of SED in DBD reactor for NO removal

HO. The most important chain breaking reactions are the formation of nitric acid (HNO₃) from the collision reaction between HO and NO₂.

In the NO/H₂O/O₂/N₂ system, the co-existence of ROS and RNS have been proved in, thus the NO can be removed through oxidation and reduction. Oxidizing agent (O, HO and HO₂) is generated from collision reaction. In terms of their oxidizing potential, HO (2.8 V) is second only to fluorine (2.87 V) and exceeds other oxidizing agents such as O₃ (2.07 V), O₂ (1.23 V), and nitric acid (0.94 V). The chain reaction involving HO radicals play an important role in the NO conversion during NTP chemical process. As shown in Figs. 5b and 7b, NO₂ concentration increases with SED increasing from 500 to 3500 J/L in H₂O/O₂/N₂ system with and without initial NO, which is different compared with that in O₂/N₂

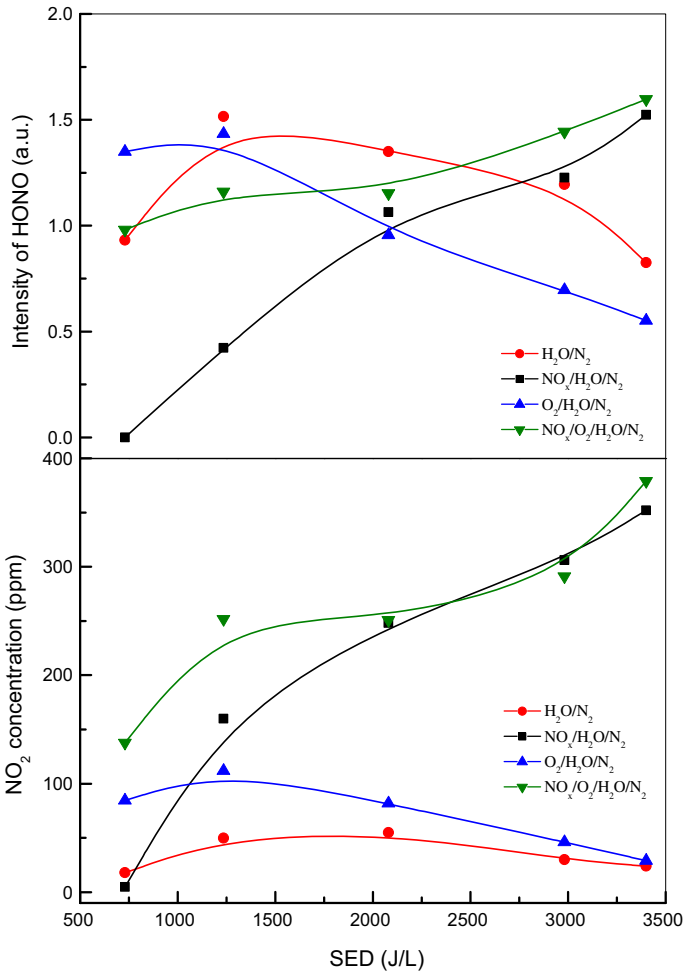


Fig. 8 NO₂ concentration and intensity of HONO spectrum

and H₂O/N₂ system. The reason for this may be that NO₂ molecules are produced from the reaction between bulk gas H₂O, O₂ and N₂.

Figure 9 shows the energy cost as a function of SED for different gas compositions. In the NO/O₂/N₂ system, the energy cost for NO conversion increase linearly with the increase of SED. In the presence of H₂O, the energy cost decreases with SED increase from 500 to 1250 J/L, then increases with further increase of SED. There are two reasons for this: the first one is that NO oxidation efficiency increase firstly then decrease with further increase of SED, the other reason is that NO is formed from bulk gas at higher SED. It seems that there is an optimal SED to achieve lowest energy cost for NO conversion (1250 J/L in this work).

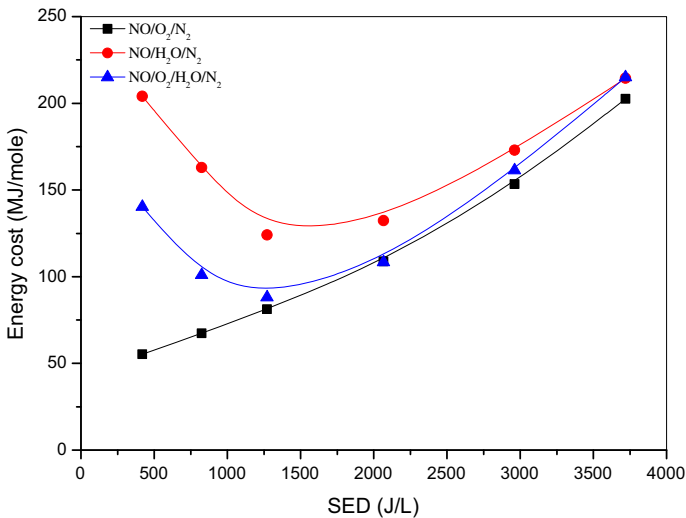


Fig. 9 Energy cost of NO conversion as a function of SED for different gas composition

NO_x Evolution and N₂O Production

Nitrogen oxides (NO_x: NO and NO₂) as a function of SED for different gas composition are shown in Fig. 10a. The quantitative gap of NO_x concentration between DBD processes with and without initial NO decreases with SED increasing from 400 to 2500 J/L. For the SED more than 2500 J/L, the difference of NO_x concentration between DBD systems with and without initial NO are maintained at a constant. For DBD process, the NTP is initiated by the collision between energetic electrons and bulk gas (H₂O, O₂ and N₂). The evolution (production or loss) of NO_x in DBD reactor is determined by the concentration of radicals and excited species such as N₂(A³Σ_u⁺), N, O, HO and NH. Since these reactive species play an important role on both formation and loss of NO_x, it is infeasible to increase products yield by unlimited increase of SED due to the product's reaction.

N₂O is a greenhouse gas and also contributes to stratospheric ozone depletion. In this section, special attention is given to N₂O. As a byproduct of NTP process, N₂O was observed in all NTP processes. N₂O concentration as a function of SED is shown in Fig. 10b. N₂O is usually considered as a by-product of NO conversion by NTP process. Zhu et al. [15] and McLarnon et al. [3] claimed that NTP alone convert NO to NO₂, then part of NO₂ will be reduced by N to form N₂O via reaction NO₂ + N → N₂O. However, the N₂O concentration decrease with NO initial concentration increasing from 0 to 500 ppm. The reason for this is that NO molecule is an excellent source for physical quenching of N₂(A³Σ_u⁺), which would suppress the N₂O formation in DBD reactor. For the NTP generated by DBD, N₂O is mainly a product from NTP process itself. The N₂O molecules are mainly formed upon collision of N₂(A³Σ_u⁺) with O₂ [33]. Partial N₂O may be formed from the reaction involving O(¹D) and NH radicals [6, 33]. The reaction rate coefficient of R14 is 3.5 × 10⁻³⁷ cm⁶/s [34]. The competing reaction route N₂ + O(¹D) → O(³P) + N₂ resulting in the quenching of O(¹D) has reaction rate coefficient of 2.5 × 10⁻¹¹ cm³/s. The NO concentration of R15 is always at ppm level. Therefore, the R13 is the dominant source of N₂O formation.

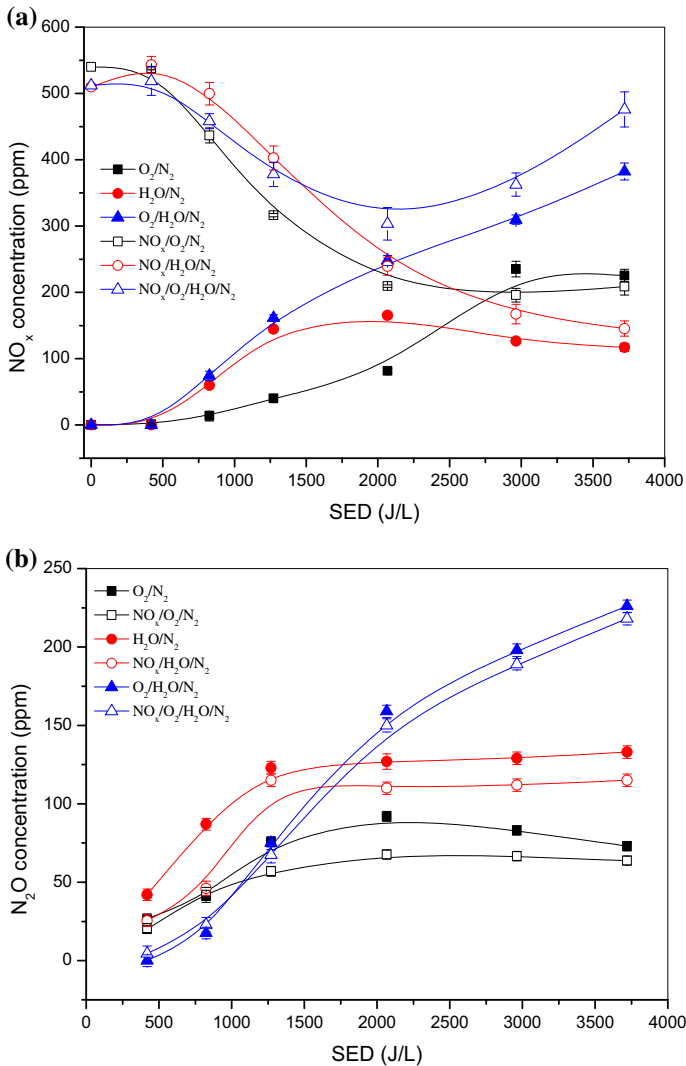
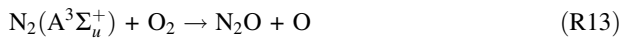
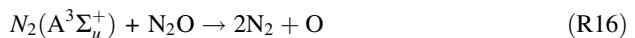
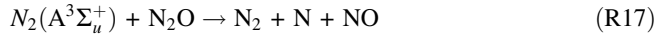


Fig. 10 NO_x concentration (a) and N₂O concentration (b) as a function of SED in DBD reactor



On the other hand, the reactive species (O(¹D) and N₂(A³Σ_u⁺)) also play an important role on N₂O conversion [33, 35].





N_2O concentration reaches a saturation with SED increasing from 500 to 1500 J/L, as shown in Fig. 10b. The N_2O concentration shows ignorable changes with SED increasing from 1500 to 3000 J/L. The reason for this may be that to $N_2(A^3\Sigma_u^+)$ plays a dual-function role on N_2O formation and loss. The increase of $N_2(A^3\Sigma_u^+)$ and N_2O concentration improves the product's reaction contributing to N_2O loss. $O(^1D)$ also plays an important role on the N_2O conversion.

Conclusion

In the DBD applications, the plasma chemistry is initiated from the collision reaction between energetic electrons and substrate molecules. The atomic oxygen (O) and hydroxyl radical (OH) generated from dissociation of O_2 and H_2O play an important role on the formation and conversion of NO, NO_2 , HNO_2 , HNO_3 and N_2O . The co-existence of different reaction pathways, such as N_2 -to-NO, NO-to- N_2 , NO-to- NO_2 , NO_2 -to-NO, N_2 -to- N_2O , NO-to- HNO_2 , NO-to- HNO_3 and HNO_2 -to- NO_2 make the DBD such a complex system. Due to interconversion of reactant and product, limitless increase of SED is not favor for energy efficiency of DBD reactor. N, O and OH can react with either reactants or products, thus leading the interconversion of N_2 and NO, NO and NO_2 , NO and HNO_2 , respectively. The byproducts N_2O was observed in all DBD process. N_2O was mainly formed by the collision reaction involving reactive species such as $N_2(A^3\Sigma_u^+)$, N, O and NH.

In the DBD systems without initial NO, the amounts of NO_x production increase with the increase of SED from 400 to 2000 J/L in the system O_2/N_2 and H_2O/N_2 . Further increase of SED will take more atomic nitrogen N into the plasma chemical process, which is favor for the NO reduction. The production of N_2O , NO_2 and HNO_2 increase with SED increasing from 500 to 3500 J/L in the system $H_2O/O_2/N_2$.

In DBD system for NO conversion, there is an optimum SED at which the best NO conversion efficiency will be obtained. NO oxidation is the main reaction pathway in the DBD process in the presence of O_2 and H_2O . NO oxidation following with absorption, adsorption or fast selective catalytic reduction is an ideal technology for NO_x removal.

Acknowledgements This study was primarily supported by National Key R&D Program of China (2017YFC0210303-01). This work was also partly supported by National Natural Science Foundation of China (21677010, U1660109).

References

1. Hessel V, Anastasopoulou A, Wang Q, Kolb G, Lang J (2013) Catal Today 211:9–28
2. Penetrante BM, Hsiao MC, Merritt BT, Vogt GE, Wallman PH (1995) IEEE Trans Plasma Sci 23:679–689

3. McLarnon CR, Penetrante BM (1998) Society of automotive engineers fall fuels and lubricants meeting 1998, San Francisco, CA, pp 19–22
4. Kossyi AYKIA, Matveyev AA, Silakov VP (1992) *Plasma Sources Sci Technol* 1:207–220
5. Fridman A, Chirokov A, Gutsol A (2005) *J Phys D Appl Phys* 38:R1–R24
6. Teodoru S, Kusano Y, Bogaerts A (2012) *Plasma Process Polym* 9:652–689
7. McLarnon CR, Penetrante BM (1998) Society of automotive engineers fall fuels and lubricants meeting, p 982434
8. Patil BS, Cherkasov N, Lang J, Ibadon AO, Hessel V, Wang Q (2016) *Appl Catal B* 194:123–133
9. Miessner H, Francke KP, Rudolph R (2002) *Appl Catal B Environ* 36:53–62
10. Tonkyn RG, Barlow SE, Hoard JW (2003) *Appl Catal B* 40:207–217
11. Atkinson R, Baulch DL, Cox RA, Hampson RF, Kerr JA, Rossi MJ, Troe J (1997) *J Phys Chem Ref Data* 26:1329
12. Fridman A (2012) *Plasma chemistry*. Cambridge University Press, New York
13. Penetrante BM, Brusasco RM, Merritt BT, Pitz WJ, Vogtlin GE, Kung MC, Kung HH, Wan CZ, Voss KE (1998) Society of automotive engineers fall fuels and lubricants meeting, p 982508
14. Fujii YAT, Yoshioka N, Rea M (2001) *J Electrostat* 51–52:8–14
15. Zhu A-M, Sun Q, Niu J-H, Xu Y, Song Z-M (2005) *Plasma Chem Plasma Process* 25:371–386
16. Jōgi I, Levoll E, Raud J (2016) *Chem Eng J* 301:149–157
17. Nakamoto K (2009) *Infrared and Raman spectra of inorganic and coordination compounds*. John Wiley & Sons, Inc., Hoboken, New Jersey
18. Hadjiivanov KI (2000) *Catal Rev* 42:71–144
19. Grundmann CTS (2009) *Int J Heat Fluid Flow* 30:394–402
20. Borgia G, Anderson CA, Brown NM (2003) *Plasma Sources Sci Technol* 12:335–344
21. Kantcheva M, Cayirtepe I (2006) *J Mol Catal A Chem* 247:88–98
22. Bibart CH, Ewing GE (1974) *J Chem Phys* 61:1284–1292
23. Cantrell CA, Davidson JA, McDaniel AH, Shetter RE, Calvert JG (1988) *Chem Phys Lett* 148:358–363
24. Guillory WA, Hunter CE (1971) *J Chem Phys* 54:598–603
25. McGraw GE, Bernitt DL, Hisatsune IC (1965) *J Chem Phys* 42:237
26. Al-Abduly A, Christensen P (2015) *Plasma Sources Sci Technol* 24:065006
27. Golde M (1988) *Int J Chem Kinet* 20:75–92
28. Wang T, Sun B-M, Xiao H-P, Wang D, Zhu X-Y, Zhong Y-F (2013) *Plasma Chem Plasma Process* 33:681–690
29. Yin S-E, Sun B-M, Gao X-D, Xiao H-P (2009) *Plasma Chem Plasma Process* 29:421–431
30. Jones LH, Badger RM, Moore GE (1951) *J Chem Phys* 19:1599
31. Eliasson B, Hirth M, Kogelschatz U (1987) *J Phys D Appl Phys* 20:1421–1437
32. Zhao G-B, Hu X, Argyle MD, Radosz M (2004) *Ind Eng Chem Res* 43:5077–5088
33. Higashi SUM, Suzuki N, Fujii K, *Trans IEEE* (1992) *Plasma Sci* 20:1–12
34. NIST chemical kinetics database. <http://kinetics.nist.gov/kinetics/index.jsp>
35. Green JHD (2001) *Plasma Chem Plasma Process* 21:459–481